Vermillion et al., http://www.jcb.org/cgi/content/full/jcb.201306071/DC1

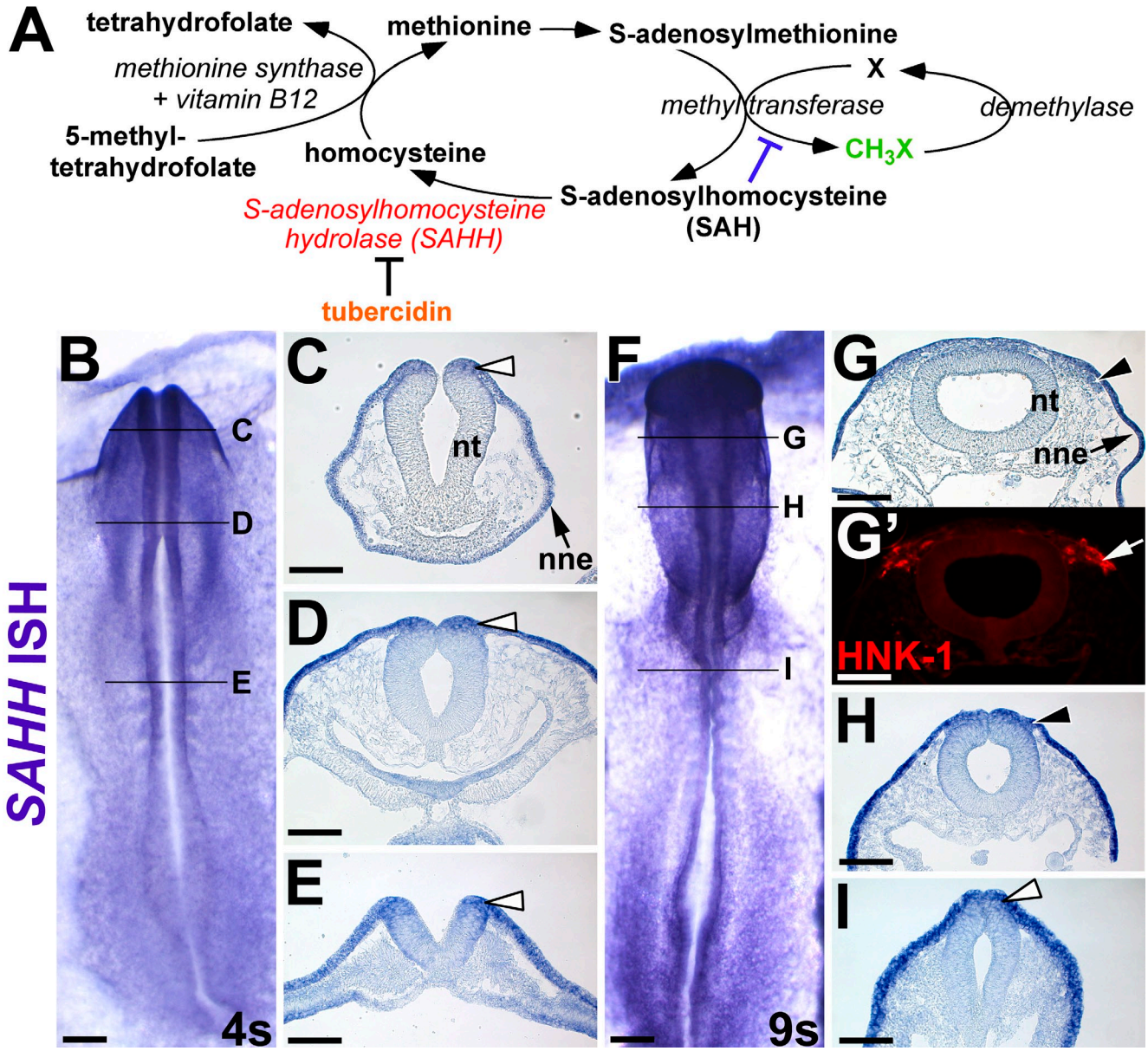

Figure S1. **SAHH, an essential enzyme of the methylation cycle, is expressed by neural crest cells.** (A) The methylation cycle. Methyltransferase-mediated transfer of a methyl group (CH_3) to a substrate (X) produces *S*-adenosylhomocysteine (SAH), which inhibits further methylation reactions. *S*-adenosylhomocysteine hydrolase (SAHH) hydrolyzes SAH, relieving the feedback inhibition. Tubercidin is a pharmacological SAHH inhibitor. (B–I) Neural crest cells express *SAHH* mRNA. Four-somite (4s, B–E) and nine-somite chick embryos (9s, F–I) sectioned at forebrain (C), midbrain (G), hindbrain (D and H), and trunk (E and I) levels. *SAHH* mRNA is widely expressed, but particularly abundant in cranial (C and D) and trunk (E and I) premigratory neural crest precursors (white arrowheads). Cranial neural crest cells maintain *SAHH* expression as they initiate migration (H), and migrate through the head mesenchyme (G; black arrowheads), expressing the neural crest marker HNK-1 (G′, white arrow). (B and F) Dorsal view; (C–E and G–I) transverse section at the level indicated in the accompanying whole mount. nne, nonneural ectoderm; nt, neural tube. Bars: (B and F) 500 µm; (all other bars) 100 µm.

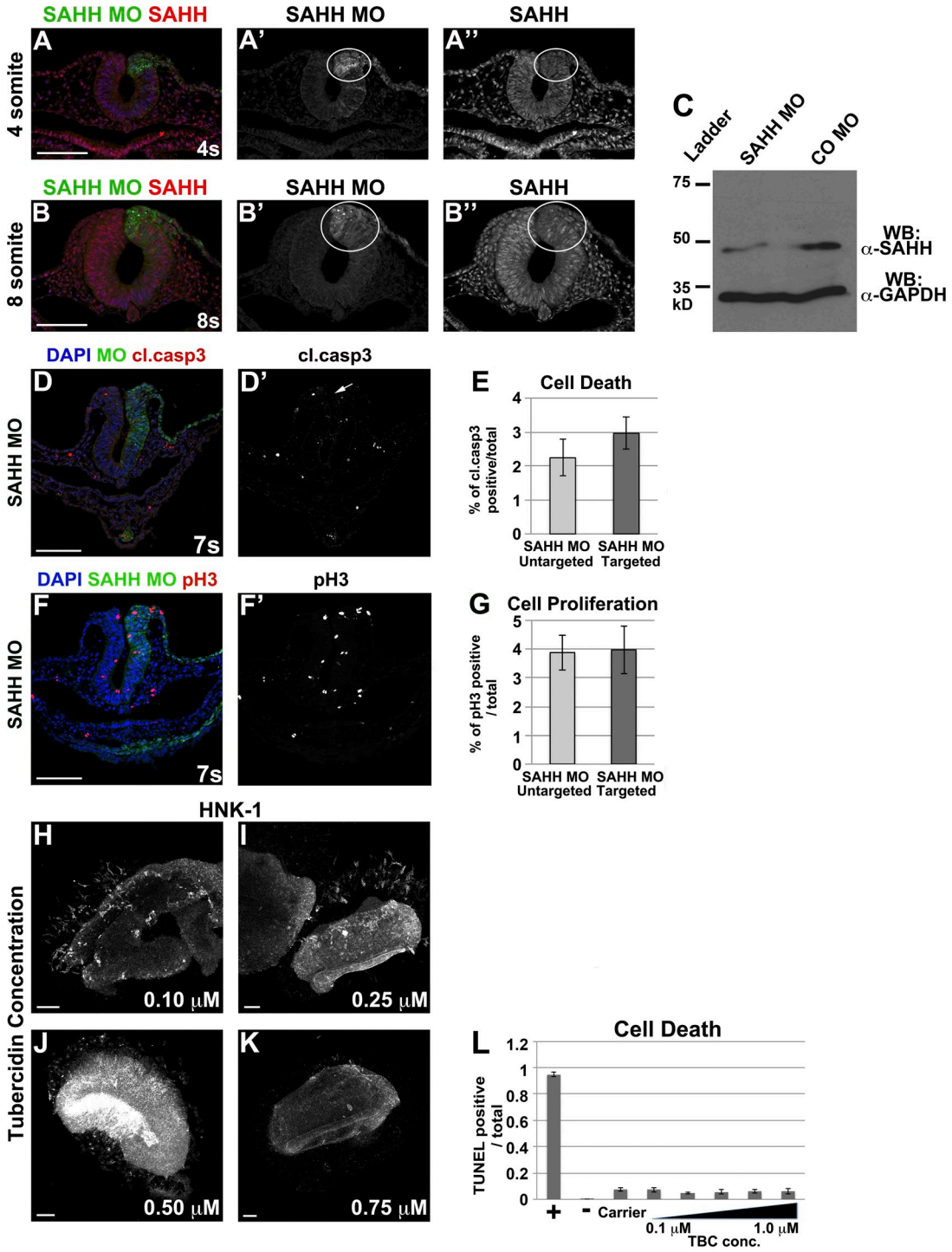

Figure S2. **SAHH MO knocks down SAHH protein levels, but blocking SAHH does not alter cell death or proliferation.** (A–C) SAHH MO–electroporated cells are deficient for SAHH protein. Embryos were unilaterally electroporated at late gastrula with SAHH MO and re-incubated to four somites (4s, A–A′′) or eight somites (8s, B–B′′ and C). (A–B) In cross sections, SAHH immunoreactivity (red, A′′ and B′′) is reduced in cells that have been targeted with SAHH MO (green, A′ and B′; cells inside circle) compared with surrounding cells (cells outside circle). (C) In Western blots of dissected, electroporated neural folds, SAHH protein levels are reduced in SAHH MO–electroporated compared with CO MO–electroporated tissue. Residual SAHH protein in SAHH MO–electroporated sample is likely due to the mosaicism of electroporation (A′ and B′) and/or perdurance of existing protein. GAPDH was used as a loading control. (D and E) SAHH knockdown does not lead to cell death. Embryos unilaterally electroporated with SAHH MO (green) at late gastrula and re-incubated to seven somites (7s) were sectioned and immunostained with anti-cleaved caspase 3 antibody (cl. casp3; red, D′) and DAPI (nucleus; blue). The percentage of cl. casp3–positive cells is not significantly different on the targeted side of the embryo compared with the untargeted side (E; P = 0.07). (F and G) SAHH knockdown does not affect proliferation. Embryos unilaterally electroporated with SAHH MO (F, green) at late gastrula and re-incubated to seven somites (7s) were sectioned and immunostained with anti–phospho-histone H3 (pH3; red, F′) and DAPI (nucleus; blue). The percentage of pH3-positive cells is not significantly different on the targeted side of the embryo compared with the untargeted side (G; P = 0.45). (H–L) Tubercidin inhibits neural crest migration in a dose-dependent manner, but does not cause cell death. (H–K) Neural tube explants were cultured in increasing concentrations of tubercidin (0.1–0.75 μM) and stained with HNK-1. Fewer HNK-1–positive neural crest cells migrate away from the neural tube with increasing concentration of tubercidin, showing dose dependency. (J) Bar graph depicting the ratio of TUNEL-positive cells to DAPI-positive cells surrounding the neural tube, showing that tubercidin does not alter the incidence of dying cells at 0.1, 0.25, 0.5, 0.75, and 1.0 μM compared with carrier treatment. Bars, 100 μm.

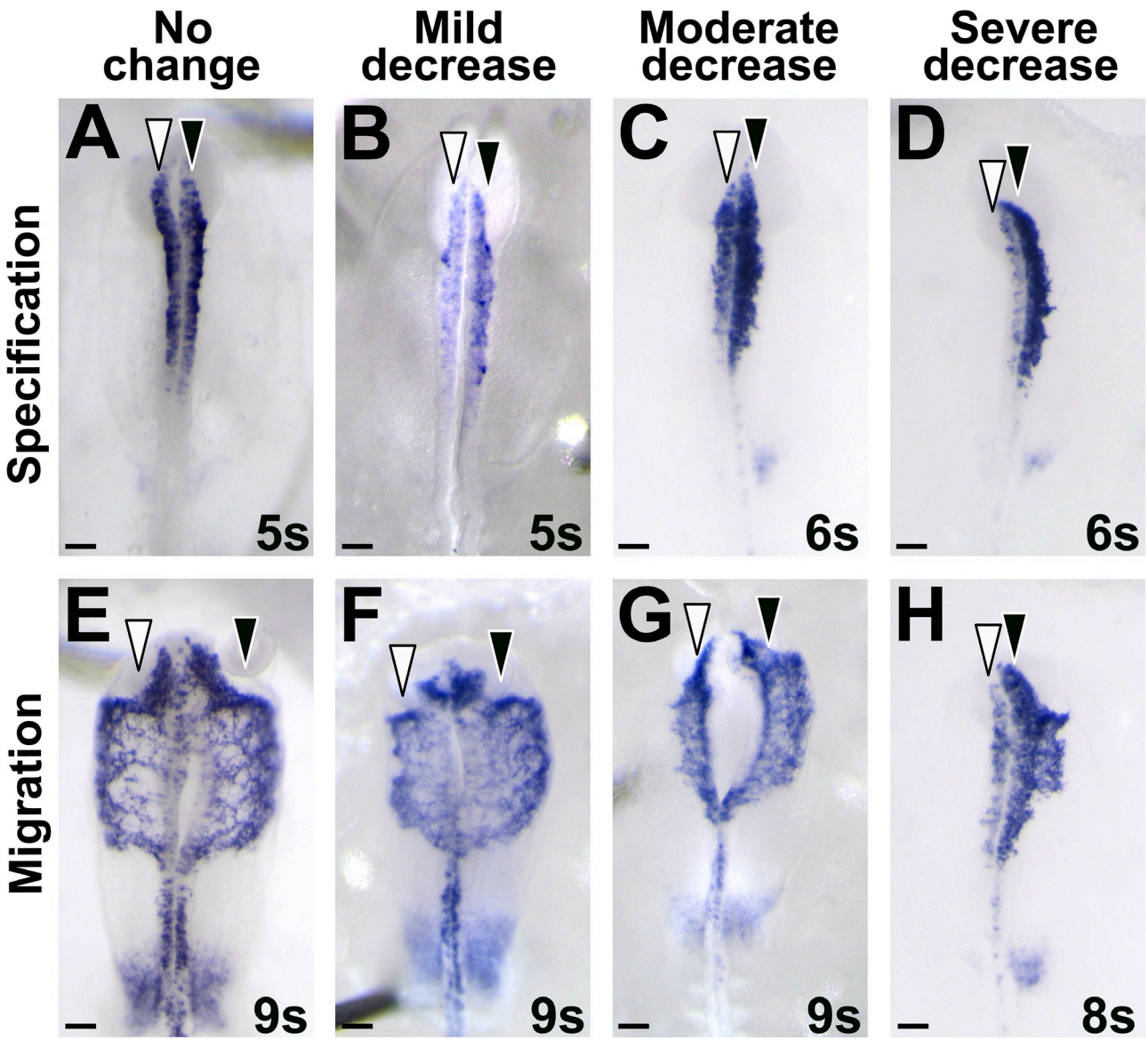

Figure S3. **Neural crest specification and migration phenotype evaluation.** (A–D) Categories of neural crest specification defects. Representative examples of embryos showing no change (A), mildly decreased (B), moderately decreased (C), or severely decreased (D) *Sox10* expression as a reflection of neural crest specification. *Snail2* expression was judged by the same criteria. (E–H) Categories of neural crest migration defects. Representative examples of embryos showing no change or equal migration (E), mildly decreased migration (F), moderately decreased migration (G), and severely decreased migration (H), using *Sox10* to visualize migratory neural crest cells. HNK-1 immunostaining was similarly judged. (A–H) Dorsal view. White arrowhead, targeted side of embryo; black arrowhead, untargeted side of embryo. Embryos shown were electroporated with SAHH MO at late gastrula, but the same categories apply to EF1α1-6xMM-GFP–electroporated embryos. Bars, 100 µm.

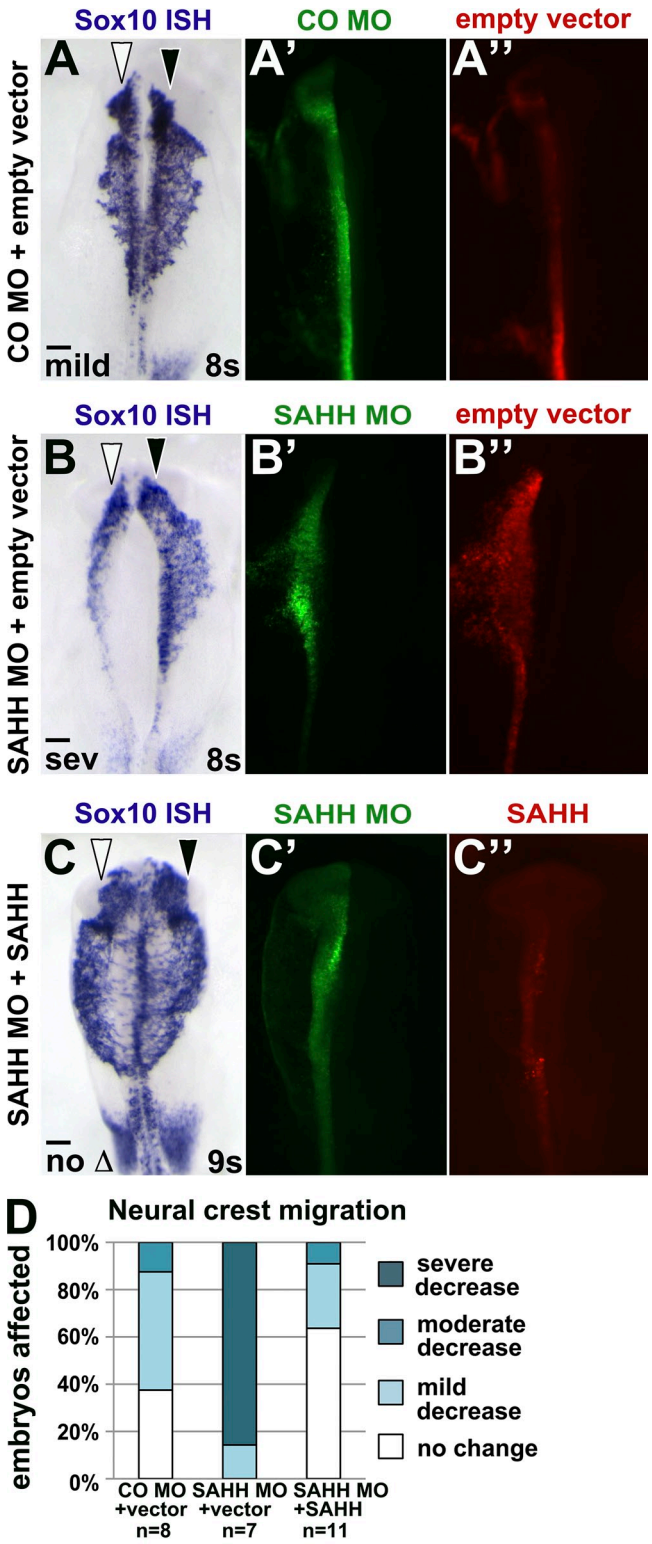

Figure S4. **Exogenous SAHH rescues SAHH knockdown, showing SAHH MO is specific.** Embryos were unilaterally electroporated with standard control MO (CO MO; A′, green) or SAHH MO (B′ and C′, green) mixed with empty pMES-mCherry expression vector (A′′ and B′′, red) or pMES-mCherry driving SAHH (C′′, red) at late gastrula. Embryos were incubated to 8–9 somites (s), and neural crest cell migration was visualized by *Sox10* in situ hybridization (purple). White arrowhead, targeted side of embryo; black arrowhead, untargeted side of embryo. (A–C) Representative embryos showing SAHH MO rescue. Neural crest migration is mildly disrupted on the targeted side when CO MO is unilaterally co-electroporated with empty pMES-mCherry (A), but is severely disrupted when SAHH MO is unilaterally co-electroporated with empty pMES-mCherry (B). Co-electroporation of SAHH MO along with 5 mg/ml pMES-SAHH-mCherry rescues SAHH knockdown so that neural crest cells migrate normally on the targeted side (C). (D) Stacked bar graph depicting the frequency and severity of migration defects in embryos co-electroporated with CO MO, SAHH MO, and pMES-mCherry expression constructs, showing that adding back SAHH rescues the migration phenotype compared with SAHH MO alone. The incidence of minimally affected control embryos may be higher than usual due to electroporation of large quantities of nucleic acid. (A–C) Dorsal views of in situ hybridization in left panel, fluorescent MO targeting in middle panel, fluorescent expression construct targeting in right panel. Bars, 100 µm.

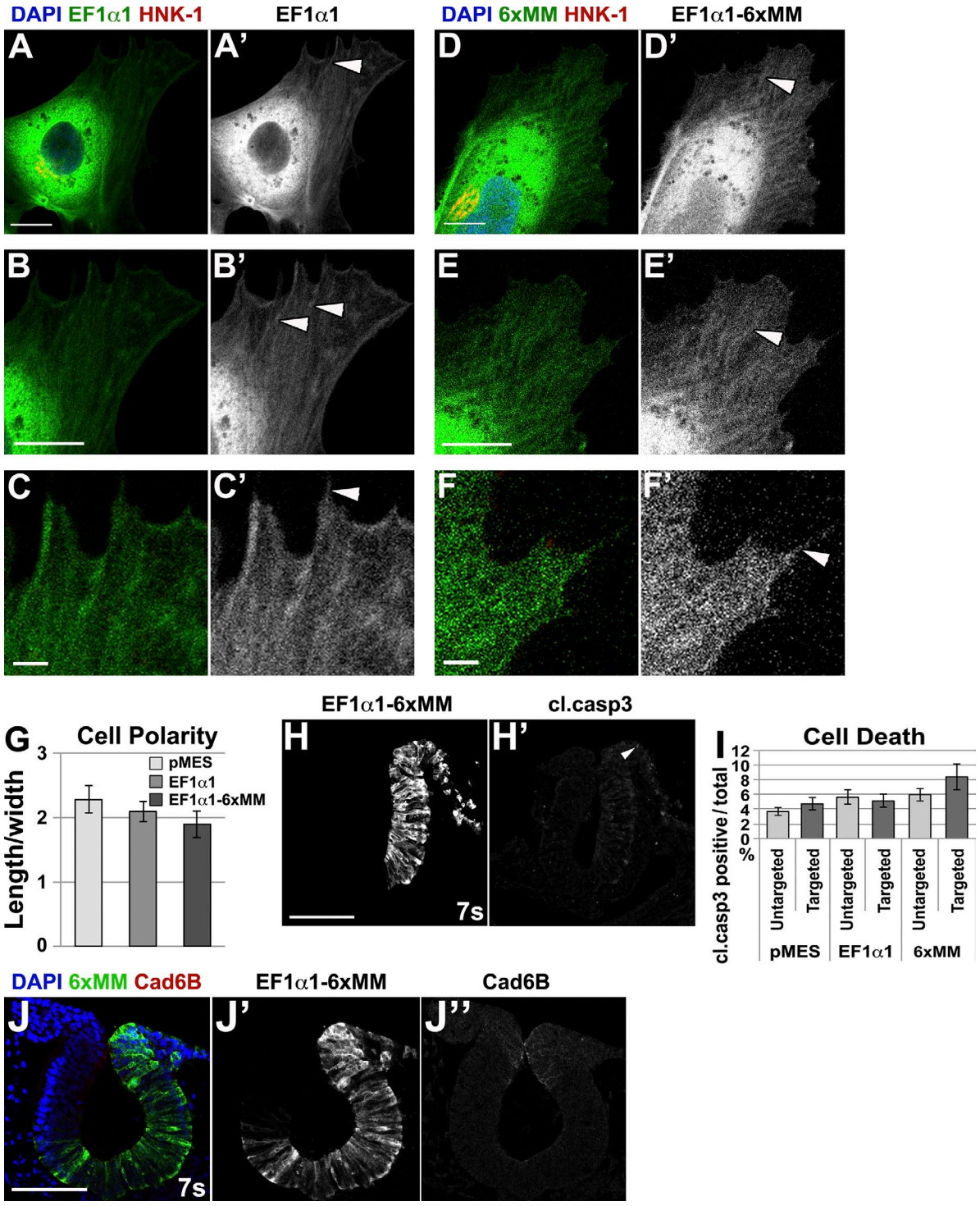

Figure S5. **EF1α1-GFP and EF1α1-6xMM-GFP localization resembles endogenous EF1α1 and does not affect cell survival.** Embryos were electroporated with EF1α1-GFP (EF1α1; A–C, green; A′–C′) or EF1α1-6xMM-GFP (EF1α1-6xMM or 6xMM; D-F, green; D′–F′) at late gastrula. (A–F) Localization of EF1α1 GFP fusions. Cranial neural folds from electroporated embryos were cultured and emigrating cells immunostained for HNK-1 (neural crest; red) and DAPI (nucleus; blue). EF1α1-GFP and EF1α1-6xMM-GFP localize in lamella (A′, B′, D′, and E′, white arrowheads) and filopodia (C′ and F′, white arrowheads) like endogenous EF1α1 (Fig. 7). (G) Cultured cranial neural crest cells that express methylation-resistant EF1α1 (EF1α1-6xMM) trend toward being less polarized than neural crest cells electroporated with empty vector (pMES) or wild-type EF1α1, though the effect is not statistically significant. (H–I) Methylation-resistant EF1α1 does not cause cell death. EF1α1-6xMM-GFP–electroporated embryos were incubated to seven somites (7s). Transverse sections were immunostained with anti-cleaved caspase 3 (cl. casp3, H′). (I) Bar graph depicting the percentage of cl. casp3–positive cells out of the total cells counted, showing that pMES, EF1α1-GFP, and EF1α1-6xMM-GFP do not significantly increase cell death on the targeted side of the embryo compared with the untargeted side ($P = 0.19$, EF1a1-6xMM). (J) EF1α1-6xMM-GFP–electroporated embryos were incubated to seven somites, and cadherin6B (Cad6B) protein visualized in midbrain transverse sections by immunofluorescence. Cad6B (J, red; J′′) is similarly down-regulated in EF1α1-6xMM-GFP–targeted (J, green; J′) and untargeted neural folds. Bars: (A, B, D, and E) 10 µm; (C and F) 1 µm; (H and J) 100 µm.

Table S1. **Putatively methylated proteins identified in a mass spectrometry proteomic screen**

Functional category/protein name	Fraction
(A) Accessory protein–adaptor/scaffold/chaperone	
Protein syndesmos	E, A
Predicted: similar to nucleoplasmin-3	A
Predicted: similar to small nuclear ribonucleoprotein Sm-D	E, A
Small nuclear ribonucleoprotein-associated protein B′	E, A
T-complex protein 1 subunit alpha	E, A
T-complex protein 1 subunit delta	E, A
T-complex protein 1 subunit theta	A
T-complex protein 1 subunit epsilon	A
T-complex protein 1 subunit zeta	A
Predicted: similar to chaperonin-containing TCP-1 complex gamma chain	A
T-complex protein 1 subunit eta	A
Heat shock cognate protein HSP-90 beta	E
Peptidylprolyl isomerase A	E
(B) Actin, cytoskeletal/cell migration	
Actin-depolymerizing factor	A
Myosin regulatory light chain 2, isoform L20-B1	A
Fibroblast alpha-actinin	A
Filamin	A
c-beta-3-beta-tubulin	A
Tropomyosin alpha 1-chain	A
Actin, cytoplasmic 2-gamma actin (Iwabata et al., 2005)	E, A
Myosin-9 (myosin heavy chain 9)	E, A
Actin, alpha skeletal muscle (Iwabata et al., 2005)	A
Myosin-10	A
Beta-actin (Iwabata et al., 2005)	A
Spectrin, alpha chain, brain	A
Tubulin-beta-7 chain	A
Tubulin-alpha-1 chain (Iwabata et al., 2005)	A
Tubulin beta-2 chain	E, A
Tubulin beta-5-chain	A
Myosin light polypeptide 6	E, A
Myosin-11	E
Elongation factor 1-alpha 1 (Ames and Niakido, 1979; Hiatt et al., 1982; Amons et al., 1983; Coppard et al., 1983; Toledo and Jerez, 1990)	E, A
(C) ATP/GTP synthesis	
ATP synthase subunit alpha, mitochondrial (Pang et al., 2010)	A
Adenine nucleotide translocator 3	E, A
ADP/ATP translocase 1	E, A
ATP-binding cassette subfamily E member 1	E, A
Guanine nucleotide-binding protein subunit beta-2-like 1	E, A
GTP-binding nuclear protein Ran	E
(D) DNA damage	
Stress 70 protein	E, A
Structural maintenance of chromosomes protein 4	E
Pre-mRNA processing factor 19	E, A
Predicted: similar to Atp51 protein	A
Heat shock protein Hsp70	E
Prohibitin	A
Cell division protein kinase 1	E
(E) ECM/intermediate filaments	
Predicted: similar to A type IV collagen	E
Vimentin	A
Lamin-B2	E, A
Collagen alpha 1CB7	A

Table S1. **Putatively methylated proteins identified in a mass spectrometry proteomic screen** *(Continued)*

Functional category/protein name	Fraction
(F) Histone protein (Young et al., 2010)	
Histone H1.10	E, A
Histone H4 type VIII (Nishioka et al., 2002)	E, A
Histone H2A.Z (Binda et al., 2013)	E, A
Histone H3.3 (Lachner et al., 2001)	A
03 H1 protein	A
Histone H2.B (Gardner et al., 2011)	E, A
(G) Metabolism	
Predicted: similar to 2,4-dienoyl-CoA reductase	E, A
C-1 tetrahydrofolate synthase, cytoplasmic	A
(H) Mitochondrial protein	
Calcium-binding mitochondrial carrier protein Aralar2	E
NADH dehydrogenase (ubiquinone) 1 alpha subcomplex subunit 9, mitochondrial	A
Predicted: similar to ATAD3A protein	E, A
Predicted: similar to dihydrolipoamide *S*-acetyltransferase	A
10-kD heat shock protein, mitochondrial	E, A
Phosphate carrier protein, mitochondrial	E, A
(I) mRNA processing	
Nuclease-sensitive element-binding protein 1	E, A
Heterogeneous nuclear ribonucleoprotein H	E
Predicted: similar to heterogeneous nuclear ribonucleoprotein U	E, A
Plasminogen activator inhibitor 1 RNA-binding protein	E
Heterogeneous nuclear ribonucleoprotein A2/B1	E
116-kD U5 small nuclear ribonucleoprotein component	A
Heterogeneous nuclear ribonucleoprotein R	E
Predicted: similar to splicing factor Prp8	E
116-kD U5 small nuclear ribonucleoprotein component	E
Predicted: similar to PTB-associated splicing factor	E
Splicing factor, arginine/serine-rich 6	E
(J) Ribonucleoprotein complex	
Synaptotagmin-binding, cytoplasmic RNA-interacting protein	E
ELAV-like protein 1	E
Predicted: similar to nuclear poly(C)-binding protein, splice variant E, partial	E
(K) Ribosomal protein	
Ribosomal protein S8	E, A
Predicted: similar to ribosomal protein L14	A
40S ribosomal protein S3	E, A
60S acidic ribosomal protein P0	E, A
Predicted: similar to Rps16 protein	E, A
Ribosomal protein S3A	A
60S ribosomal protein L7	E, A
Predicted: similar to ribosomal protein L14	E, A
60S ribosomal protein L4 (Pang et al., 2010)	E, A
60S ribosomal protein L3 (Pang et al., 2010)	E, A
60S ribosomal protein L22	E, A
Predicted: similar to ribosomal protein L18a	A
60S ribosomal protein L7a	E, A
40S ribosomal protein S4	E, A
Ribosomal protein S8	A
Ribosomal protein L10A (Carroll et al., 2008)	E, A
40S ribosomal protein S6	A
Predicted: similar to 40S ribosomal protein S2	E, A
Predicted: similar to ribosomal protein S25	E, A
60S ribosomal protein L6	A
Predicted: similar to ribosomal protein L8	E, A
Predicted: similar to ribosomal protein L18	E, A

Table S1. **Putatively methylated proteins identified in a mass spectrometry proteomic screen** *(Continued)*

Functional category/protein name	Fraction
Predicted: similar to Rpl24 protein	A
Predicted: similar to ribosomal protein S15 isoform 2	A
60S ribosomal protein L27 (Pang et al., 2010)	E, A
Ribosomal protein L30	E, A
40S ribosomal protein S13 (Pang et al., 2010)	A
40S ribosomal protein S11	E, A
40S ribosomal protein S14	E, A
60S ribosomal protein L36 (Carroll et al., 2008)	E, A
Predicted: similar to HL23 ribosomal protein	E, A
Predicted: similar to ribosomal protein S20	E, A
40S ribosomal protein S17 (Pang et al., 2010)	A
Predicted: similar to Rpl17 protein	A
60S ribosomal protein L37A	A
40S ribosomal protein S6	E, A
Ribosomal RNA processing protein 1 homolog B	E
Predicted: similar to ribosomal protein S15 isoform 2	E
Predicted: similar to Rpl24 protein	E
Ribosomal L1 domain containing 1	E
60S ribosomal protein L6	E
60S ribosomal protein L19	E
60S ribosomal protein L7-like 1	E
Predicted: similar to ribosomal protein L15	E
40S ribosomal protein S12	E
Predicted: similar to ribosomal protein L38	E
Predicted: similar to Rpl123a protein	A
60S ribosomal protein L35	A
(L) Ribosome biogenesis	
Nucleolar GTP-binding protein 1 (Pang et al., 2010)	E
Nucleolar protein 56	E
Predicted: similar to pescadillo	E
Predicted: similar to chromosome 1 open reading frame 33	E
(M) RNA-binding protein, localized translation	
Cold-shock domain containing protein E1	E, A
Fragile X mental retardation syndrome-related protein 1	E
Insulin-like growth factor 2 mRNA binding protein 3	E
Insulin-like growth factor 2 mRNA-binding protein 1	E, A
Double-stranded RNA-binding protein Staufen homologue 1	E
(N) RNA helicase	
ATP-dependent RNA helicase DDX1-dead box protein 1	A
ATP-dependent RNA helicase DDX3X	E, A
Probable ATP-dependent RNA helicase DDX5	E, A
ATP-dependent RNA helicase DDX1	E
DEAH (Asp-Glu-Ala-His) box polypeptide 15	E
(O) Transcriptional regulation	
Prohibitin-2	A
Heat-shock cognate 71-kD protein	E, A
Activating transcription factor 7–interacting protein 1	E
(P) Translational regulation	
Elongation factor 1-beta	E
Protein lin-28 homologue A	E
Bifunctional aminoacyl-tRNA synthetase	E, A
Eukaryotic translation elongation factor 1	E, A
Elongation factor 2	E, A
Polyadenylate-binding protein 1	E, A
Aspartyl-tRNA synthetase, cytoplasmic	E, A
Arginyl-tRNA synthetase, cytoplasmic	E, A

Table S1. **Putatively methylated proteins identified in a mass spectrometry proteomic screen** *(Continued)*

Functional category/protein name	Fraction
Eukaryotic translation initiation factor 2 subunit 3	A
Elongation factor 1-beta	A
Eukaryotic translation initiation factor 2 subunit 1	A
Cysteinyl-tRNA synthetase, cytoplasmic	E
Predicted: similar to eukaryotic translation elongation factor 1 delta	E
Lysyl-tRNA synthetase	E
Eukaryotic translation initiation factor 6	E
(Q) Transmembrane protein	
Uncharacterized protein KIAA0090 homologue	A
Predicted: similar to transmembrane protein 93 isoform 2	E
(R) Vesicular trafficking	
Predicted: similar to isoleucyl-tRNA synthetase	A
Predicted: similar to beta prime cop	E, A
Vesicle-associated membrane protein–associated protein A	A
(S) Yolk precursors	
Vitellogenin-2	E
Vitellogenin-1	E
(T) Miscellaneous	
Anti-thrombin — blood coagulation	E
Cytoplasmic activation proliferation-associated protein 1 — cell proliferation	E
Nucleophosmin — diverse cellular processes	E, A
Tubulin-tyrosine ligase-like protein 12 — ligase activity	E
Nucleolin — main nucleolar protein	E, A
Predicted: similar to endothelial-monocyte activating polypeptide 11 — proinflammatory cytokine	A
Predicted: similar to NOL1 protein — putative RNA methyltransferase	E
Peroxiredoxin-1 — Redox regulation	A
(U) Unknown	
Predicted: similar to DNA segment, Chr 10, Wayne State University 52, expressed	A
Predicted: similar to sec61-like protein	A
Predicted: similar to WW domain binding protein II	E
Predicted: similar to KIAA0432	E
Predicted: similar to KIAA1931 protein	E
Predicted: similar to Gu protein	E
Predicted: similar to LOC495253	E, A

The results of proteomic analysis to identify neural crest cytoplasmic proteins containing mono- and di-methylated lysines. Proteins listed were identified by two or more peptides at 95% confidence. Proteins are classified into functional categories and labeled if they were identified from emigrating (E) or actively migrating (A) neural crest cells.

References

Ames, G.F., and K. Niakido. 1979. In vivo methylation of prokaryotic elongation factor Tu. *J. Biol. Chem.* 254:9947–9950.

Amons, R., W. Pluijms, K. Roobol, and W. Möller. 1983. Sequence homology between EF-1 alpha, the alpha-chain of elongation factor 1 from Artemia salina and elongation factor EF-Tu from *Escherichia coli*. *FEBS Lett.* 153:37–42. http://dx.doi.org/10.1016/0014-5793(83)80115-X

Binda, O., A. Sevilla, G. LeRoy, I.R. Lemischka, B.A. Garcia, and S. Richard. 2013. SETD6 monomethylates H2AZ on lysine 7 and is required for the maintenance of embryonic stem cell self-renewal. *Epigenetics*. 8:177–183. http://dx.doi.org/10.4161/epi.23416

Carroll, A.J., J.L. Heazlewood, J. Ito, and A.H. Millar. 2008. Analysis of the Arabidopsis cytosolic ribosome proteome provides detailed insights into its components and their post-translational modification. *Mol. Cell. Proteomics*. 7:347–369. http://dx.doi.org/10.1074/mcp.M700052-MCP200

Coppard, N.J., B.F. Clark, and F. Cramer. 1983. Methylation of elongation factor 1 alpha in mouse 3T3B and 3T3B/SV40 cells. *FEBS Lett.* 164:330–334. http://dx.doi.org/10.1016/0014-5793(83)80311-1

Gardner, K.E., L. Zhou, M.A. Parra, X. Chen, and B.D. Strahl. 2011. Identification of lysine 37 of histone H2B as a novel site of methylation. *PLoS ONE*. 6:e16244. http://dx.doi.org/10.1371/journal.pone.0016244

Hiatt, W.R., R. Garcia, W.C. Merrick, and P.S. Sypherd. 1982. Methylation of elongation factor 1 alpha from the fungus Mucor. *Proc. Natl. Acad. Sci. USA*. 79:3433–3437. http://dx.doi.org/10.1073/pnas.79.11.3433

Iwabata, H., M. Yoshida, and Y. Komatsu. 2005. Proteomic analysis of organ-specific post-translational lysine-acetylation and -methylation in mice by use of anti-acetyllysine and -methyllysine mouse monoclonal antibodies. *Proteomics*. 5:4653–4664. http://dx.doi.org/10.1002/pmic.200500042

Lachner, M., D. O'Carroll, S. Rea, K. Mechtler, and T. Jenuwein. 2001. Methylation of histone H3 lysine 9 creates a binding site for HP1 proteins. *Nature*. 410:116–120. http://dx.doi.org/10.1038/35065132

Nishioka, K., J.C. Rice, K. Sarma, H. Erdjument-Bromage, J. Werner, Y. Wang, S. Chuikov, P. Valenzuela, P. Tempst, R. Steward, et al. 2002. PR-Set7 is a nucleosome-specific methyltransferase that modifies lysine 20 of histone H4 and is associated with silent chromatin. *Mol. Cell*. 9:1201–1213. http://dx.doi.org/10.1016/S1097-2765(02)00548-8

Pang, C.N., E. Gasteiger, and M.R. Wilkins. 2010. Identification of arginine- and lysine-methylation in the proteome of *Saccharomyces cerevisiae* and its functional implications. *BMC Genomics*. 11:92. http://dx.doi.org/10.1186/1471-2164-11-92

Toledo, H., and C.A. Jerez. 1990. In vivo and in vitro methylation of the elongation factor EF-Tu from *Euglena gracilis* chloroplast. *FEMS Microbiol. Lett.* 59:241–246. http://dx.doi.org/10.1111/j.1574-6968.1990.tb03830.x

Young, N.L., P.A. Dimaggio, and B.A. Garcia. 2010. The significance, development and progress of high-throughput combinatorial histone code analysis. *Cell. Mol. Life Sci.* 67:3983–4000. http://dx.doi.org/10.1007/s00018-010-0475-7